ADVANCED ENERGY MATERIALS
www.advenergymat.de

Sponge-Like Piezoelectric Polymer Films for Scalable and Integratable Nanogenerators and Self-Powered Electronic Systems

*Yanchao Mao, Ping Zhao, Geoffrey McConohy, Hao Yang, Yexiang Tong, and Xudong Wang**

Nanogenerators (NGs) are an emerging technology that uses piezoelectric nanomaterials to efficiently and effectively harvesting mechanical energy from ambient sources on the nanometer scale.[1–3] Because of the superior mechanical and electromechanical properties of nanoscale structures, NGs have demonstrated promising capability in scavenging energy from mechanical deflections,[4] acoustic waves,[5–7] fluid or air flows,[8,9] and even human activities.[10] Currently, the output of NGs has reached the sub-milliwatt level, which is sufficient to power many small electronic devices, including light-emitting diodes (LEDs),[4] laser diodes,[11] pH sensors,[12] UV sensors,[12] speed/weight sensors,[13] and toxic pollutant sensors.[14] The piezoelectric output of NGs was also used to directly drive electrochemical reactions including lithium ion intercalation,[15] electrodegradation of dyes,[16] and electrochemical water splitting.[17] This research illustrated the possibility of realizing self-powered electronic systems, which is a greatly desired concept for developing care-free sensor networks, implantable biomedical devices, and next-generation personal electronics. To date, most demonstrations of NG prototypes rely on bending, deflection, or vibration of the piezoelectric components to harvest mechanical energy. These processes require considerably large open spaces, and thus may not be practical in many circumstances of ambient mechanical energy harvesting and is a challenge to seamlessly integrate with many electronic devices. New designs are needed to realize practical and effective NG operations in common daily environments. Furthermore, fabrication of NGs typically relies on the integration of a tremendous amount of nanostructure building blocks, which remains a critical obstacle for scaling up the NG manufacturing. Therefore, for a practical and integratable NG, the functional piezoelectric material should be easily fabricated in large scale and highly integratable with other electronic devices.

β-Phase polyvinylidene fluoride (PVDF) is the most broadly studied piezoelectric polymer material.[18–20] Due to its high piezoelectric coefficient, excellent stability, and desirable flexibility, nanostructured PVDF polymer has been used in a variety of NG designs for mechanical energy harvesting.[8,9,15,21–23] For instance, PVDF nanowires fabricated by electrospinning showed an enhanced mechanical energy conversion efficiency.[22] By integrating PVDF polymer with an electrochemical system, a self-charging power cell was fabricated as a sustainable power source.[15] The biocompatible nature of PVDF allows it to be applied to harvest energy inside biological systems[8] and from human respiration.[9] Combined with its high mechanical resistance, dimensional stability, and chemical stability, the flexible PVDF polymer holds good potential for integratable NGs in self-powered electronic systems.

In order to enhance the piezoelectric performance, PVDF should possess well controlled nanomorphology, high purity of the β-phase, and excellent flexibility and durability. Moreover, a facile method for fabricating large-area nanostructured piezoelectric PVDF NG is desired. Here, we report a novel sponge-like mesoporous piezoelectric PVDF thin-film structure for NG development. The mesoporous PVDF thin films were fabricated using a simple casting-etching process in the wafer scale. The mesoporous PVDF NGs can be directly attached to the surface of an electronic device (e.g., a cell phone) and effectively convert mechanical energy from ambient surface oscillations to electricity using the device's own weight to enhance the amplitude. Multiple PVDF NGs can be readily integrated and operate synchronically to raise the output power for the operation of electronic devices. This technique is scalable and integratable, providing a promising solution for developing practical self-powered electronic devices.

The mesoporous PVDF thin film was fabricated by casting a mixture of PVDF solution and ZnO nanoparticles (NPs) onto a flat surface, followed by HCl acid solution etching to remove

Y. C. Mao, Prof. X. D. Wang
Department of Materials Science and Engineering
University of Wisconsin-Madison
Madison, WI, 53706, USA
E-mail: xudong@engr.wisc.edu
Y. C. Mao, H. Yang, Prof. Y. X. Tong
MOE Laboratory of Bioinorganic and Synthetic Chemistry
KLGHEI of Environment and Energy Chemistry
School of Chemistry and Chemical Engineering
Sun Yat-sen University
Guangzhou, 510275, China
Prof. P. Zhao
Department of Mechanical and Industrial Engineering
University of Minnesota-Duluth
Duluth, MN, 55812, USA
G. McConohy
Department of Engineering Physics
University of Wisconsin-Madison
Madison, WI, 53706, USA

DOI: 10.1002/aenm.201301624

ADVANCED ENERGY MATERIALS
www.advenergymat.de

Materials Views
www.MaterialsViews.com

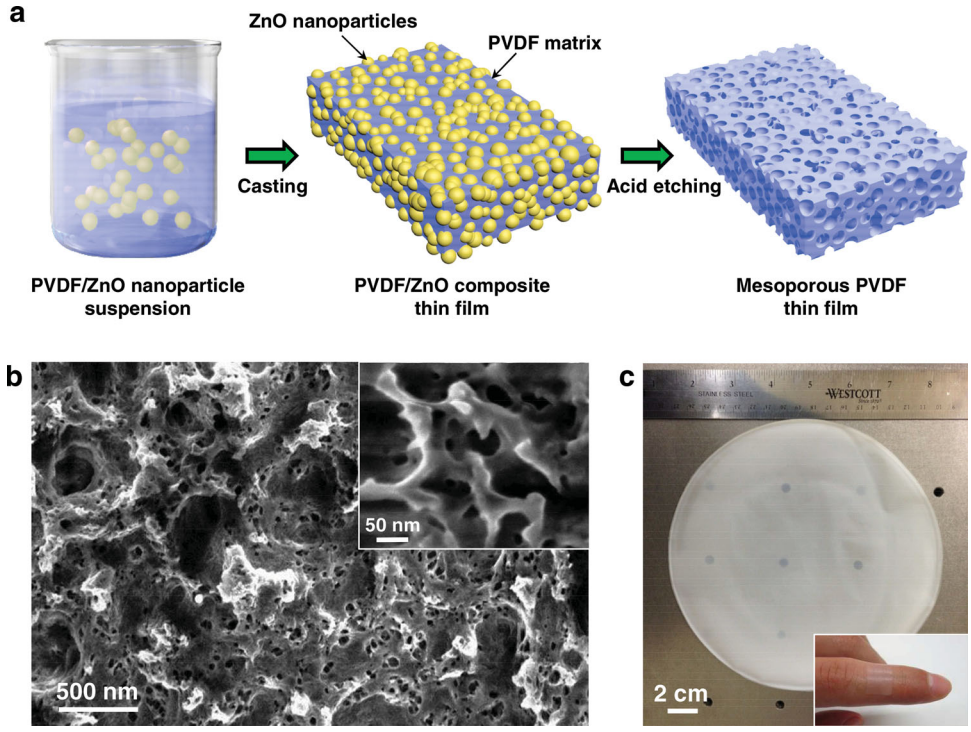

Figure 1. Processing and structure of mesoporous PVDF thin films. a) Schematic procedure for fabricating mesoporous piezoelectric PVDF thin films. b) SEM image of a mesoporous PVDF thin film fabricated from a ZnO-PVDF mixture with 50% ZnO mass fraction. The inset is a higher-magnification SEM image showing that the pore size matches ZnO NP size. c) A photograph of an as-fabricated wafer-scale mesoporous PVDF thin film (18.5 cm in diameter). The inset shows a small piece of the mesoporous PVDF thin film well adhered to the finger surface.

ZnO (**Figure 1**a). HCl solution was selected because PVDF is a hydrophobic polymer with excellent chemical stability against corrosive solvents including acids.[24,25] Introducing ZnO NPs to PVDF has two purposes: 1) to create porosity in the PVDF film to modulate its mechanical property; and 2) to seed the formation of the piezoelectric β-phase. Additionally, ZnO has several unique advantages compared to other inorganic (e.g., SiO_2) or organic (e.g., polystyrene) NP templates for the fabrication of porous nanomaterials, including low-cost, non-toxicity, good scalability, and facile removal by acidic solution.[26–30] Scanning electron microscopy (SEM) images (Figure 1b) show the sponge-like mesoporous structure of the PVDF thin film after removing ZnO NPs. The pore sizes are consistent with those of the ZnO NPs (35–45 nm in average, inset of Figure 1b and Supporting Information Figure S1). The pores are interconnected allowing ZnO NPs to be completely removed via chemical etching. This was evidenced by the energy dispersive X-ray spectroscopy (EDS) spectrum where only C and F elements were detected (Figure S2, Supporting Information). Fourier transform infrared (FTIR) spectrum was used to confirm the crystal phase of the mesoporous PVDF thin film. The characteristic peaks of the β-phase at 509, 840 and 1280 cm^{-1} can be clearly observed in the FTIR spectrum (Figure S3, Supporting Information).[31,32] The formation of β-phase PVDF can be attributed to the interactions between the PVDF dipoles and surface charges on ZnO surfaces. In wurtzite ZnO crystals, the (0001) surfaces are terminated with Zn cations and always positively charged, while the $(000\bar{1})$ surfaces are O-terminated and exhibit negative charges.[33] The intrinsic ZnO polar surfaces could interact with the PVDF CF_2 or CH_2 groups that have negative and positive charge densities, respectively, and thus initiated the β-phase nucleation. This mechanism is consistent with the surface charge-induced crystallization phenomenon that has been discovered in many PVDF composites with fillers such as $BaTiO_3$,[34] clays,[35–37] hydrated ionic salts,[38] polymethylmethacrylate (PMMA),[39] TiO_2,[40] ferrite,[40] Pd,[41] Au,[42] and carbon nanotubes.[43,44]

Using this method, a large-area mesoporous PVDF thin film (18.5 cm in diameter) was fabricated (Figure 1c), demonstrating the capability of producing high quality piezoelectric polymer thin films in large scales. The film thickness can be facilely adjusted by the amount of casting mixture. The as-fabricated thin film was translucent, soft, and very flexible. It can be seamlessly attached to rough and curvy surfaces, such as human skin (inset of Figure 1c).

The mesoporous PVDF film provides an excellent platform for developing integratable NGs, which only need two layers of metal electrodes (Cu foil in our case) to be attached to both sides of the film. The simple design ensures high volume power density of the NGs. The flexible thin film configuration allows the NG to be directly attached to electronic devices and uses the device's own weight as the proof mass to amplify the oscillation of the PVDF film. In our experiment, a piece of aluminum block was used in place of an electronic device to test the energy harvesting ability (see setup details in the Experimental Section). As schematically shown in **Figure 2**a, a PVDF NG (2 cm × 1 cm × 28 μm) with an aluminum block (65 g) was placed on a flat surface. An oscillator was located 6 cm

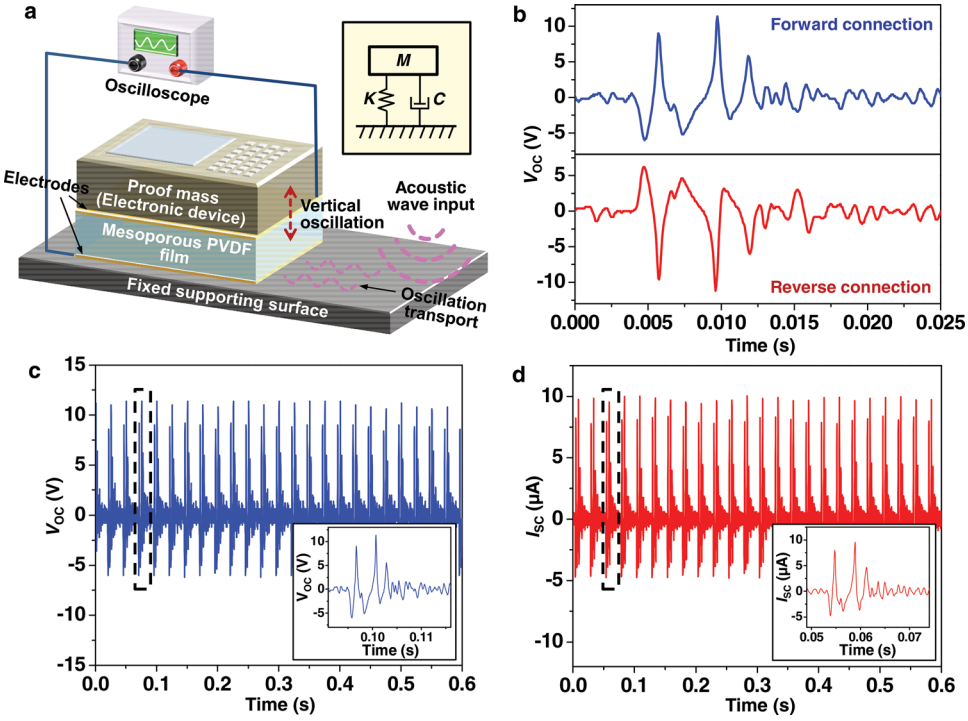

Figure 2. Characterization of PVDF thin film NGs. a) Schematic setup for characterizing PVDF thin film NGs for harvesting mechanical energy from surface oscillations. The mesoporous PVDF thin film-weight system can be simplified as a free vibration system with damping, as shown in the inset. b) The voltage output of a PVDF thin film NG (fabricated from a 50% ZnO mass fraction mixture) generated during one cycle of surface oscillation. The blue and red curves were collected under forward and reverse connections, respectively. c,d) The voltage (c) and current (d) output of the PVDF NG under continuous surface oscillation. Insets show the output curve features during one cycle of surface oscillation.

away from the NG system and generated surface oscillations with a controlled frequency. The oscillations were transported across surface and created a slight up-and-down motion of the aluminum block. Thus, the PVDF NG located in-between was pressed accordingly and produced piezoelectric output. Here, the PVDF-weight system can be simplified as a free vibration system with damping (inset of Figure 2a). The open-circuit voltage (V_{OC}) of the NG under the forward and reverse connections was measured during the oscillation. The upper panel of Figure 2b shows the V_{OC} signal generated during one surface oscillation cycle (the driving oscillator was operated at 40 Hz). In the case of reverse connection, the V_{OC} demonstrated identical amplitude with reversed polarization (the lower panel of Figure 2b), which confirmed the genuineness of the piezoelectric output signals. Figure 2c,d show the V_{OC} and short-circuit current (I_{SC}) of the NG, respectively, when the supporting surface was oscillating at 40 Hz. The average peak values of the V_{OC} and I_{SC} were found to be about 11.0 V and 9.8 μA, respectively. This output performance was higher than the recently reported values for other PVDF based NGs, such as single PVDF nanofiber (30 mV/3 nA, 6.5 μm diameter/600 μm length),[22] PVDF nanofibers (20 mV/0.3 nA, sample thickness and area were not indicated),[8] PVDF film (0.4 V, 1.5 μm thickness, output current was not indicated),[45] PVDF mats (≈1 V, 100 μm thickness/1 cm^2 area, output current was not indicated),[46] porous PVDF film (1.3 V/0.3 μA, 5 μm thickness/1 cm^2 area),[23] PVDF nanofiber membranes (≈2.2 V/≈4.5 μA, 140 μm thickness/2 cm^2 area),[47] PVDF microbelts(≈6 V, 26 μm thickness, output current was not indicated).[9] As shown in the insets of Figure 2c,d, within one surface oscillation cycle, the output signal peaked and quickly dropped to the base level, indicating large damping of the PVDF film like a sponge layer. The NG was able to work over a long period of time under a constant oscillation without noticeable degradation in the output signal (Figure S4, Supporting Information).

Porosity is an important feature that controls the mechanical energy harvesting ability of the mesoporous PVDF films. To investigate the porosity effect, PVDF thin films with different porosities were prepared from mixtures with a series of ZnO mass (or volume) fractions (Figure S5, Supporting Information). The V_{OC} of these mesoporous PVDF thin films with identical thicknesses (28 μm) was measured at a frequency of 40 Hz, and their peak values were plotted as a function of porosity (**Figure 3**a). The peak V_{OC} increased from 3.5 V to 11.0 V as the porosity increased from 6.5% to 32.6% (ZnO mass fraction increased from 10% to 50%), and then decreased to 8.3 V as the porosity further increased to 45.5% (ZnO mass fraction increased to 70%). The optimal porosity for achieving the maximum V_{OC} output was identified to be ≈11.0 V. The porosity-output relationship was found directly related to the amount of β-phase PVDF. Meanwhile, the total amount of PVDF per unit volume decreased as the ZnO ratio increased. As evidenced by FTIR spectra (Figure S6, Supporting Information), the amount of α-phase in as-prepared PVDF films monotonically decreased as the ZnO ratio increased. The amount of β-phase increased as the ZnO mass ratio increased from 10% to 50%, and then

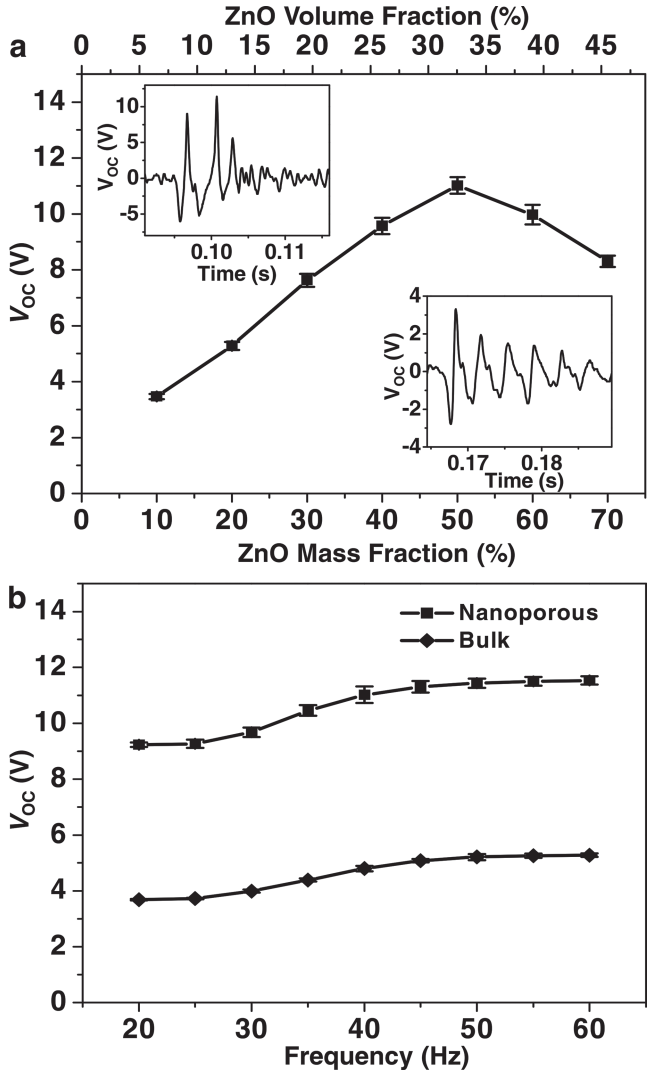

Figure 3. Porosity-related voltage output. a) The peak voltage measured from PVDF thin film NGs as a function of porosity (or ZnO volume/mass fraction). All the voltage data were collected from 40 Hz surface oscillation. The upper and lower insets show the detailed voltage output features generated during one cycle of surface oscillation from mesoporous PVDF thin films fabricated using 50% and 10% ZnO mass fraction mixtures, respectively. More rapid signal decay can be observed from the 50% ZnO sample. b) Comparison of the peak voltages between a mesoporous PVDF thin film (50% ZnO mass fraction) and a solid β-phase PVDF thin film obtained under surface oscillation frequencies from 20 to 60 Hz. The voltage outputs show a relatively stable value within the testing frequency range (increase at 30 Hz is due to the increase of oscillator driving power). The output of mesoporous PVDF thin film was more than two times higher than that of the solid PVDF thin film.

decreased when the ZnO mass fraction further increased. The mesoporous PVDF film made from the mixture of 50% ZnO (by mass) possessed the maximum β-phase quantity, corresponding to the highest piezoelectric potential.

In addition, PVDF films with different porosities yielded different oscillation patterns, which also contributed to the electrical output variation. The upper and lower insets of Figure 3a show the voltage output signal generated in one oscillation cycle, from the mesoporous PVDF thin films prepared using the 50% and 10% ZnO mass fraction mixtures, respectively. The 10%-ZnO sample generated a series of oscillating signals and relatively slowly decayed from ≈3 V to ≈1 V within ≈20 ms. The 50%-ZnO sample produced significantly higher output (≈11 V), which quickly decayed to the base line within ≈10 ms. To further understand the porosity-related performance, the mechanical properties, specifically the spring constant (K) and damping coefficient (C), were calculated based on the oscillation patterns (Figure S8, Supporting Information) for PVDF thin films with different porosity (Figure S5, Supporting Information). Both experimental and calculation results agreed that PVDF thin films with higher porosity (>40% ZnO) were soft and lossy like a sponge, while lower porosity PVDF thin films were still more like a rigid plastic film. Therefore, under the same amount of external impact, the sponge-like high-porosity PVDF thin films would yield considerably larger displacement, and thus produced much higher electrical output. Comparing the calculated data (Table S1, Supporting Information), the spring constant decreased by 60–70% when the ZnO ratio increased to >40%; meanwhile, the overall damping coefficient only increased by ≈10%. Therefore, although more mechanical energy was dissipated mechanically in the higher porosity PVDF films, a good portion of it was converted into electrical energy due to the larger film displacement (higher C_{total} including higher electrical damping component).

Since the mesoporous PVDF NGs were operated under forced oscillation conditions with large output (their resonance frequencies were in the kHz range), the higher damping ratio can ensure all the input mechanical energy were dissipated prior to the following impact. With part of the dissipated mechanical energy being converted into electricity, the output can remain a constant high value across a relatively wide frequency range. For a 50%-ZnO PVDF NG, V_{OC} were measured within a frequency range from 20 to 60 Hz, which are common oscillation frequencies in ambient environments. It was found that the piezoelectric output was nearly independent to the agitation frequency (Figure S9, Supporting Information) and the maximum V_{OC} remained between 9.2–11.5 V (square dots in Figure 3b, the slight increase after 30 Hz was due to necessary input power increase of the oscillator).

In general, combination of high β-phase ratio and sponge-like mechanical property made the mesoporous PVDF thin films a promising candidate for harvesting mechanical energy from surface oscillations. This advantage is clearly illustrated by comparing the performances of mesoporous PVDF thin films with solid β-phase PVDF thin films that were prepared[48] and tested within the same frequency range and under the same oscillation power. The same size solid PVDF film produced peak V_{OC} from 3.7 V to 5.3 V (diamond dots in Figure 3b), which was over two times smaller than that produced by the mesoporous PVDF films.

To demonstrate the application potential as a direct current (DC) power source, a mesoporous PVDF NG was connected to a capacitor (22 μF) through a full-wave bridge circuit, as shown by the equivalent circuit in the inset of **Figure 4**a. The alternating current (AC) piezoelectric output was fully rectified through the bridge circuit (Figure S10, Supporting Information). Figure 4a illustrates the charging process of the capacitor under different

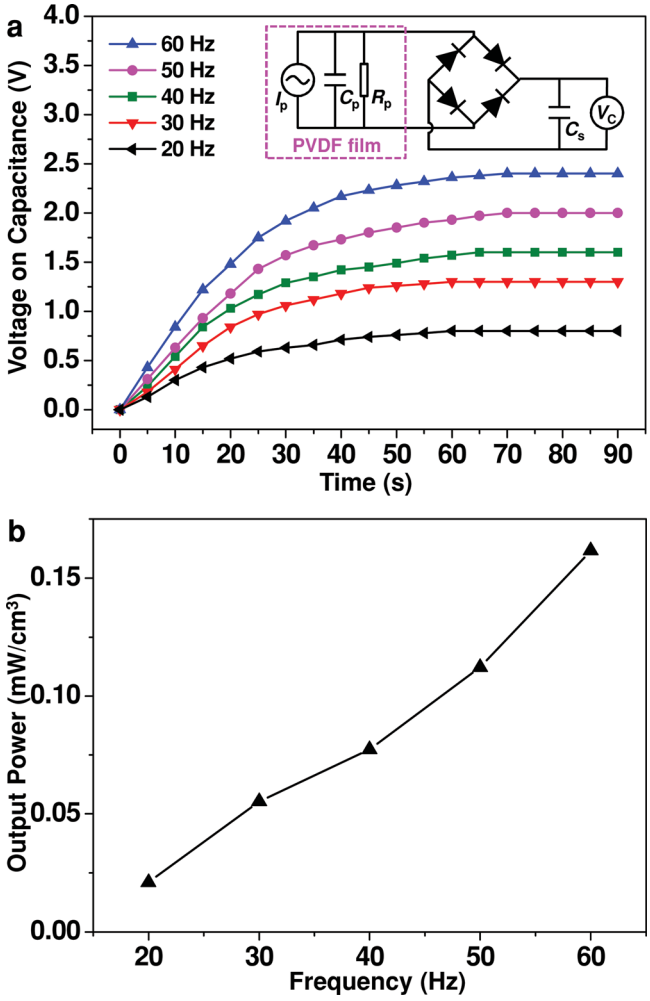

Figure 4. Characterization of frequency-related energy output. a) Voltages measured across a 22 μF capacitor when it was charged by a mesoporous PVDF thin film NG (from 50% ZnO mass fraction mixture) under different surface oscillation frequencies. Inset is the equivalent circuit. b) The output power density calculated from the capacitor charging curves as a function of the surface oscillation frequency.

agitation frequencies. Higher frequency yielded higher saturation voltage of the capacitor, which is a result of equilibrium established between the NG's charging rate and the capacitor's leakage rate. The voltage held by the capacitor reached 2.4 V in 70 s under an oscillation frequency of 60 Hz. Based on the charging curves, the output power of the mesoporous PVDF NG was calculated via the equation: $P = CU^2/2t$, where C is the capacitance of the capacitor, U is the saturation voltage, and t is the time for the voltage to reach the saturation point. This was the practical power output on the specific capacitor. It monotonically increased as a function of oscillation frequency from 0.02 mW cm^{-3} to 0.16 mW cm^{-3} at 60 Hz (Figure 4b).

Another unique merit of the mesoporous PVDF NG is its excellent integratability. Because it does not require additional component to fulfill the energy harvesting function, multiple NGs can be simply integrated into one system and operate with identical phase and frequency. This feature allows direct multiplication of NGs' AC output without rectifying them first. In order to demonstrate this merit, two PVDF NGs were fabricated and attached to the same aluminum block. When operated under 40 Hz, the peak V_{OC} and I_{SC} output of NG I and NG II was 11.1 V, 9.7 μA (**Figure 5**a) and 11.0 V, 9.8 μA (Figure 5b), respectively. By connecting these two NGs in serial, the peak V_{OC} output increased to 20.2 V, which was approximately the sum of the peak V_{OC} of each NGs. Meanwhile, the peak I_{SC} output was barely affected (9.3 μA) and only 4.1% drop was observed in comparison to the lower peak I_{SC} (9.7 μA) of the two individual NGs (Figure 5c). For parallel connection as shown in Figure 5d, the peak I_{SC} was largely increased to 17.5 μA, which was only 10.3% less than the sum of the peak I_{SC} of both NGs. Meanwhile the peak V_{OC} remained at nearly the same individual level (10.5 V). The loss of output could be attributed to the leakage of electric charge through the connection circuit.[10] This result revealed that PVDF NG integration followed the general rules of battery connection, although their outputs were in AC form.

The excellent integratability allows direct application of the PVDF NGs onto the surface of an electronic device and operation by the device's own weight. As a demonstration, four PVDF NGs (1 × 2 cm^2 each) were attached to the back of a smart phone, as shown in Figure 5e. These NGs were connected in parallel. The phone was then placed on a flat wood surface where an oscillator was placed ≈10 cm away (the same setup for testing PVDF NGs, Figure 5f). When the oscillator was turned on, the phone followed the surface oscillation and NGs underneath were activated by the phone's weight to convert the surface oscillating mechanical energy to electricity (see Video S1, Supporting Information). The output power was rectified by a bridge circuit and stored in capacitors. 3.7 V was reached on a 47 μF capacitor by this phone-NG setup, and the corresponding charging curve is shown in Figure S11 (Supporting Information). Connecting two capacitors in series after they were charged in parallel could yield high enough electrical energy to activate the turning on of the phone by itself (i.e., the phone battery was active; Video S2, Supporting Information). This demonstrated the promising application potential of the mesoporous PVDF thin films as a supportive energy source for powering personal electronics using ambient mechanical energy sources.

In conclusion, we successfully demonstrated a novel integratable NG design based on sponge-like mesoporous piezoelectric PVDF thin films. This type of NG can generate considerable electrical energy by harvesting mechanical energy from surface oscillations. Compared to previous developments of NGs, the mesoporous PVDF thin film NG possesses several unique merits that are critical for harvesting ambient mechanical energy and developing practical self-powered electronic systems. First, the method is very simple and effective for large-scale fabricating mesoporous piezoelectric PVDF thin films. This fabrication method also circumvents the requirement of large mechanical strain or high electric field for the formation of β-phase PVDF. This is a highly desired feature for manufacturing practical and industrial-level NGs. Second, the NG uses the electronic device's own weight to modulate its displacement and amplify its electrical output. This unique operation principle realizes a very simple system design. It

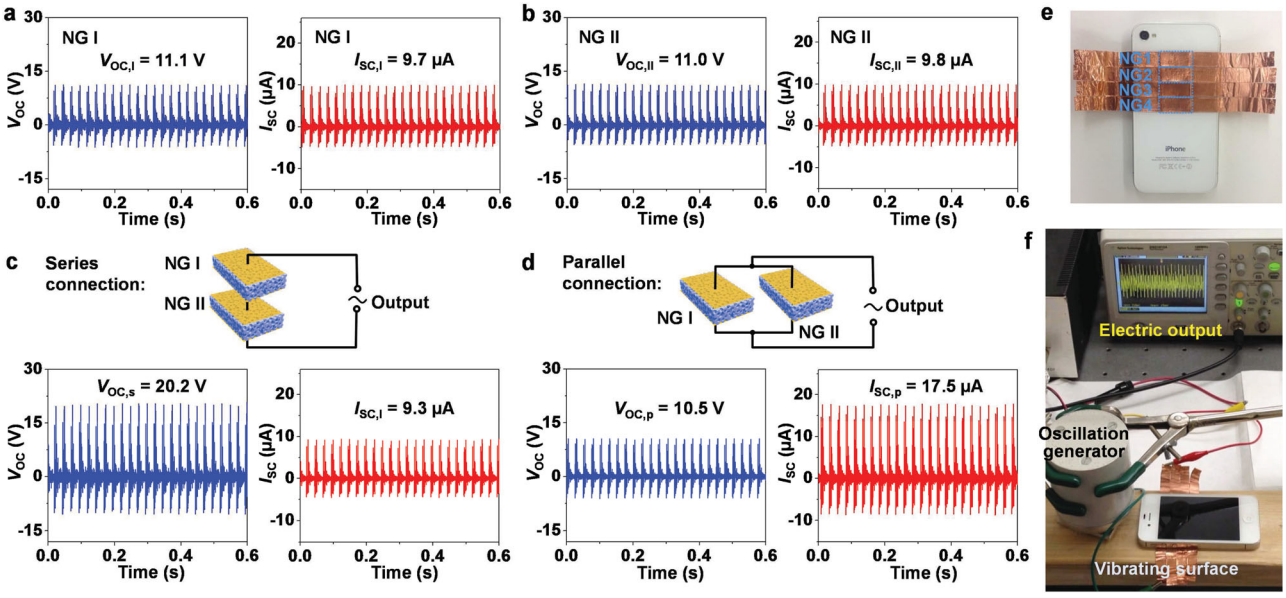

Figure 5. Operation demonstration of mesoporous PVDF thin film NGs. a,b) Voltage and current outputs of two individual NGs, I and II, respectively. c,d) Voltage and current outputs measured from NGs I and II when they were connected in series (c) and in parallel (d), respectively. Corresponding connection conditions are shown in the top insets. e) A photograph of four mesoporous PVDF thin film NGs (1×2 cm^2 each) attached on the back side of a smart phone. They were connected in parallel. f) Operation of the integrated phone-NG system driven by surface oscillation, and the electrical output was recorded by the oscilloscope.

also provides an ideal solution for directly integrating multiple NGs into one system to boost the output without rectifying or synchronizing individual signals. Third, the controllable nanoporosity enables adjustable mechanical property of the PVDF films. At high porosity, the PVDF film acts as a flexible and soft sponge. Although the high-porosity films would dissipate more mechanical energy, a good portion of it could be converted into electrical energy due to the large film displacement resulting in large electric output under small surface oscillations. Last, the forced oscillation allows the PVDF NG to be operated away from its resonant frequency with large outputs. This unique feature opens another route toward broad-band mechanical energy harvesting. Integrating the PVDF NGs with a smart phone demonstrated the unique merits discussed above. It provides a promising solution for developing practical self-powered personal electronic devices.

Experimental Section

Fabrication of Mesoporous PVDF Thin Films: PVDF powder (Sigma Aldrich) was dissolved in *N*,*N*-dimethylformamide (DMF) solvent (10 wt%) at 65 °C and then mixed with ZnO NPs (35–45 nm, US Research Nanomaterials, Inc.). The mass ratio between ZnO NPs to PVDF was adjusted to create different porosity. The mixture was treated in ultrasonic bath for 30 min and yielded a uniformly-mixed PVDF/ZnO NP suspension. The suspension was cast into a film shape in a petri dish and dried in atmosphere at 75 °C. The films were then immersed in a 37 wt% HCl solution for 3 h to completely remove the ZnO NP template. After acid etching, the films were washed by deionized (DI) water and mesoporous PVDF thin films were obtained.

PVDF NG Design and Testing: The morphology and structure of the PVDF thin films were characterized using a LEO 1530 scanning electron microscope. FTIR characterizations of the PVDF films were performed by the Bruker Tensor 27 spectrometer. To make a PVDF NG, the mesoporous PVDF thin film was cut into 1×2 cm^2 pieces. Both sides of the PVDF thin film were taped with Cu foils as electrodes. The PVDF film was then poled at room temperature in an oil bath. An electric field of 60 V μm^{-1} was applied between the top and bottom Cu electrodes for 2 h. The PVDF samples were stable throughout the entire poling process. No short circuit or noticeable voltage fluctuation was detected. The poled PVDF NG was taped on the bottom surface of a piece of aluminum block (65 g), which was used in place of an electronic device. The aluminum block was placed on a flat wood surface. The surface oscillation was generated by an oscillator located ≈6 cm away from the aluminum block. The oscillator impacted the wood surface with a controlled frequency. The electrical output signal from the PVDF NG was recorded by an Agilent DSO1012A oscilloscope.

Supporting Information

Supporting Information is available from the Wiley Online Library or from the author.

Acknowledgements

The authors thank M. B. Starr and C. J. Tao for providing their phones for our experiments. X.W. thanks the support of DARPA under grant No. N66001-11-1-4139, Air Force under award FA9550-13-1-0168, and National Science Foundation CMMI-1148919. Y.M. thanks the China Scholarship Council for financial support. Y.T. thanks the support of NSFC (21273290) and the Research Fund for the Doctoral Program of Higher Education of China (No.20120171110043).

Received: October 24, 2013
Revised: November 24, 2013
Published online: January 27, 2014

[1] Y. F. Hu, L. Lin, Y. Zhang, Z. L. Wang, *Adv. Mater.* **2012**, *24*, 110.
[2] G. Zhu, A. C. Wang, Y. Liu, Y. S. Zhou, Z. L. Wang, *Nano Lett.* **2012**, *12*, 3086.
[3] X. D. Wang, *Nano Energy* **2012**, *1*, 13.
[4] K. I. Park, M. Lee, Y. Liu, S. Moon, G. T. Hwang, G. Zhu, J. E. Kim, S. O. Kim, D. K. Kim, Z. L. Wang, K. J. Lee, *Adv. Mater.* **2012**, *24*, 2999.
[5] X. D. Wang, J. H. Song, J. Liu, Z. L. Wang, *Science* **2007**, *316*, 102.
[6] S. N. Cha, J. S. Seo, S. M. Kim, H. J. Kim, Y. J. Park, S. W. Kim, J. M. Kim, *Adv. Mater.* **2010**, *22*, 4726.
[7] J. H. Lee, K. Y. Lee, B. Kumar, N. T. Tien, N. E. Lee, S. W. Kim, *Energy Environ. Sci.* **2013**, *6*, 169.
[8] B. J. Hansen, Y. Liu, R. S. Yang, Z. L. Wang, *ACS Nano* **2010**, *4*, 3647.
[9] C. L. Sun, J. Shi, D. J. Bayerl, X. D. Wang, *Energy Environ. Sci.* **2011**, *4*, 4508.
[10] M. Lee, C. Y. Chen, S. Wang, S. N. Cha, Y. J. Park, J. M. Kim, L. J. Chou, Z. L. Wang, *Adv. Mater.* **2012**, *24*, 1759.
[11] S. Xu, B. J. Hansen, Z. L. Wang, *Nat. Commun.* **2010**, *1*. 97.
[12] S. Xu, Y. Qin, C. Xu, Y. G. Wei, R. S. Yang, Z. L. Wang, *Nat. Nanotechnol.* **2010**, *5*, 366.
[13] L. Lin, Y. F. Hu, C. Xu, Y. Zhang, R. Zhang, X. N. Wen, Z. L. Wang, *Nano Energy* **2013**, *2*, 75.
[14] M. Lee, J. Bae, J. Lee, C. S. Lee, S. Hong, Z. L. Wang, *Energy Environ. Sci.* **2011**, *4*, 3359.
[15] X. Y. Xue, S. H. Wang, W. X. Guo, Y. Zhang, Z. L. Wang, *Nano Lett.* **2012**, *12*, 5048.
[16] Y. Yang, H. L. Zhang, S. Lee, D. Kim, W. Hwang, Z. L. Wang, *Nano Lett.* **2013**, *13*, 803.
[17] M. B. Starr, J. Shi, X. D. Wang, *Angew. Chem. Int. Ed.* **2012**, *51*, 5962.
[18] P. Ueberschlag, *Sens. Rev.* **2001**, *21*, 118.
[19] L. Yu, P. Cebe, *Polymer* **2009**, *50*, 2133.
[20] P. Martins, C. Cparros, R. Goncalves, P. M. Martins, M. Benelmekki, G. Botelho, S. Lanceros-Mendez, *J. Phys. Chem. C* **2012**, *116*, 15790.
[21] M. A. Rahman, B.-C. Lee, D.-T. Phan, G.-S. Chung, *Smart Mater. Struct.* **2013**, *22*, 085017.
[22] C. E. Chang, V. H. Tran, J. B. Wang, Y. K. Fuh, L. W. Lin, *Nano Lett.* **2010**, *10*, 726.
[23] S. Cha, S. M. Kim, H. Kim, J. Ku, J. I. Sohn, Y. J. Park, B. G. Song, M. H. Jung, E. K. Lee, B. L. Choi, J. J. Park, Z. L. Wang, J. M. Kim, K. Kim, *Nano Lett.* **2011**, *11*, 5142.
[24] J. Kong, K. Li, *J. Appl. Polym. Sci.* **2001**, *81*, 1643.
[25] S. J. Oh, N. Kim, Y. T. Lee, *J. Membr. Sci.* **2009**, *345*, 13.
[26] A. L. Wang, H. Xu, J. X. Feng, L. X. Ding, Y. X. Tong, G. R. Li, *J. Am. Chem. Soc.* **2013**, *135*, 10703.
[27] L. X. Ding, A. L. Wang, G. R. Li, Z. Q. Liu, W. X. Zhao, C. Y. Su, Y. X. Tong, *J. Am. Chem. Soc.* **2012**, *134*, 5730.
[28] D. A. Bernards, T. A. Desai, *Adv. Mater.* **2010**, *22*, 2358.
[29] S. I. Na, S. S. Kim, W. K. Hong, J. W. Park, J. Jo, Y. C. Nah, T. Lee, D. Y. Kim, *Electrochim. Acta* **2008**, *53*, 2560.
[30] J. Qiu, W. Yu, X. Gao, X. Li, *Nanotechnology* **2006**, *17*, 4695.
[31] A. Salimi, A. A. Yousefi, *Polym. Test.* **2003**, *22*, 699.
[32] J. F. Zheng, A. H. He, J. X. Li, C. C. Han, *Macromol. Rapid Commun.* **2007**, *28*, 2159.
[33] Z. L. Wang, X. Y. Kong, J. M. Zuo, *Phys. Rev. Lett.* **2003**, *91*, 185502.
[34] H. Ye, W. Shao, L. Zhen, *J. Appl. Polym. Sci.* **2013**, *129*, 2940.
[35] T. U. Patro, M. V. Mhalgi, D. V. Khakhar, A. Misra, *Polymer* **2008**, *49*, 3486.
[36] D. Shah, P. Maiti, E. Gunn, D. F. Schmidt, D. D. Jiang, C. A. Batt, E. P. Giannelis, *Adv. Mater.* **2004**, *16*, 1173.
[37] L. Priya, J. P. Jog, *J. Polym. Sci., Part B: Polym. Phys.* **2002**, *40*, 1682.
[38] M. Benz, W. B. Euler, O. J. Gregory, *Macromolecules* **2002**, *35*, 2682.
[39] Z. Shi, J. Ma, C. W. Nan, *J. Electroceram.* **2008**, *21*, 390.
[40] P. Martins, X. Moya, L. C. Phillips, S. Kar-Narayan, N. D. Mathur, S. Lanceros-Mendez, *J. Phys. D: Appl. Phys.* **2011**, *44*, 482001.
[41] D. Mandal, K. J. Kim, J. S. Lee, *Langmuir* **2012**, *28*, 10310.
[42] W. Wang, S. Zhang, L. O. Srisombat, T. R. Lee, R. C. Advincula, *Macromol. Mater. Eng.* **2011**, *296*, 178.
[43] S. S. Yu, W. T. Zheng, W. X. Yu, Y. J. Zhang, Q. Jiang, Z. D. Zhao, *Macromolecules* **2009**, *42*, 8870.
[44] P. Martins, A. C. Lopesa, S. Lanceros-Mendez, *Prog. Polym. Sci.* DOI: 10.1016/j.progpolymsci.2013.07.006.
[45] D. Y. Lee, H. Kim, H. M. Li, A. R. Jang, Y. D. Lim, S. N. Cha, Y. J. Park, D. J. Kang, W. J. Yoo, *Nanotechnology* **2013**, *24*, 175402.
[46] D. Dhakras, V. Borkar, S. Ogale, J. Jog, *Nanoscale* **2012**, *4*, 752.
[47] J. Fang, X. Wang, T. Lin, *J. Mater. Chem.* **2011**, *21*, 11088.
[48] S. Satapathy, S. Pawar, P. K. Gupta, K. B. R. Varma, *Bull. Mater. Sci.* **2011**, *34*, 727.